IOP Publishing Superconductor Science and Technology
Supercond. Sci. Technol. 31 (2018) 065010 (6pp) https://doi.org/10.1088/1361-6668/aac05d

Anomalous reduction in the long-time flux creep relaxation in superconducting $Ca_{10}(Pt_4As_8)((Fe_{1-x}Pt_x)_2As_2)_5$ ($x \approx 0.05$) single crystals

N Haberkorn[1,2], Silu Huang[3] and R Jin[3]

[1] Comisión Nacional de Energía Atómica and Consejo Nacional de Investigaciones Científicas y Técnicas, Centro Atómico Bariloche, Av. Bustillo 9500, 8400 San Carlos de Bariloche, Argentina
[2] Instituto Balseiro, Universidad Nacional de Cuyo, Av. Bustillo 9500, 8400 San Carlos de Bariloche, Argentina
[3] Department of Physics and Astronomy, Louisiana State University, Baton Rouge, LA 70803, United States of America

E-mail: nhaberk@cab.cnea.gov.ar

Received 27 February 2018, revised 17 April 2018
Accepted for publication 26 April 2018
Published 11 May 2018

Abstract

We report the vortex dynamics of superconducting a $Ca_{10}(Pt_4As_8)((Fe_{1-x}Pt_x)_2As_2)_5$ ($x \approx 0.05$) single crystal with $T_c = 26$ K investigated by performing magnetic measurements. The field dependence of the magnetization displays a second peak (SPM), typically related to a crossover between elastic and plastic vortex relaxation in a weak pinning scenario. Long-time flux creep relaxation measurements for fields smaller that of the SPM show that the vortex dynamics can be separated in two different regions. For magnetic fields smaller than the lower end of the SPM, glassy relaxation (with a characteristic glassy exponent μ) is observed. For magnetic fields between the lower end and the SPM, the flux creep rate decreases systematically to values below to the ones predicted by the collective theory. This effect can be understood by considering a stable vortex lattice configuration. As the field position of the SPM can be adjusted by modifying the quenched potential, our results suggest that extremely low flux creep relaxation rate may be tuned in many other superconducting materials.

Keywords: iron based superconductors, vortex dynamics, glassy exponents

(Some figures may appear in colour only in the online journal)

1. Introduction

Among the fascinating and widely studied features of superconductors are their time-dependent magnetic properties. In particular, information about the flux creep rate (decay of the persistent critical current densities J_c) is highly required from both a basic understanding and an application point of view. The vortex motion in type-II superconductors is mainly governed by thermal fluctuations and quenched disorder. The strength of vortex fluctuations is related to the Ginzburg number $Gi = \frac{1}{2}\left[\frac{\gamma T_c}{H_c^2(0)\xi^3(0)}\right]^2$ ($H_c(0)$ is the thermodynamic critical field at $T = 0$ K, T_c critical temperature, γ anisotropy, and $\xi(0)$ the coherence length at $T = 0$ K). The simplest phenomenological parameter to describe the strength of disorder is the critical current–density ratio (J_c/J_0) (where J_0 is the depairing current density) [1]. In conventional low-T_c materials (LTS), $Gi \approx 10^{-8}$ and the flux creep rate is governed by a standard Anderson–Kim process. However, the situation is different for iron based superconductors (IBS, with $Gi \approx 10^{-5}$–10^{-2}) and for high-temperature cuprates (HTS, with $Gi > 0.01$), in which the short coherence length, the large anisotropy and the high critical temperature generate great thermal fluctuations [2, 3]. In LTS, the thermal effects

produce an almost negligible and essentially logarithmic temporal decay of the persistent current. In IBS and HTS, such decay is much larger and displays non-logarithmic behavior (which is related to the elastic nature of the flux lines). Such behavior has been explained considering that the decay of the persistent current with time is determined by the current dependence of the activation energy:

$$U\,(J) = \left(\frac{U_0}{\mu}\right)\left[\left(\frac{J_c}{J}\right)^{\mu} - 1\right], \tag{1}$$

where $\mu > 0$ is the glassy exponent and U_0 is the characteristic pinning energy. The decay of J with time t is given by the interpolation between the classical Anderson–Kim model and the logarithmic term:

$$J = J_c\left[1 + \frac{\mu T}{U_0}\ln(t/t_0)\right]^{-1/\mu}, \tag{2}$$

where t_0 is a characteristic time and T is the temperature. The normalized relaxation rate is:

$$S = -\frac{\mathrm{d}(\ln J)}{\mathrm{d}(\ln t\,)} = \frac{T}{U_0 + \mu T\ln(t/t_0)} = \frac{T}{U_0}\left(\frac{J}{J_c}\right)^{\mu}. \tag{3}$$

The condition $\mu > 0$ implies a diverging activation energy as $J \to 0$ in equation (1), which is the consequence of elastic creep. The glassy exponent μ is regime dependent. The collective creep model predicts $\mu = 1/7$ for single vortex creep, $3/2$ or $5/2$ for small bundles, and $7/9$ for large bundles in random point disorder regimes whereas different μ is expected for correlated disorder in various single vortex and collective regimes [1].

The concept of glassy relaxation governed by vortex bundles has been largely applied to the study of different families of Fe-based superconductors with anisotropy ranging from low γ (i.e., FeSe) [4, 5] to high γ (i.e., $SmFeAsO_{0.85}F_{0.15}$) [6]. The field dependence of the magnetization is characterized by a second peak in the magnetization (SPM) or fishtail [7–10]. This phenomenon was previously found in $YBa_2Cu_3O_{7-\delta}$ single crystals, and was attributed to the elastic (vortex bundles at low fields [11]) and plastic crossover [3]. In addition, a first order phase transition has been noticed, which varies from an ordered (elastically pinned) low-field vortex phase (Bragg-glass), to a high-field disordered phase characterized by the presence of topological defects [12]. While its origin is unclear, SPM usually appears in superconductors with random disorder. For example, the SPM tends to disappear after detwinnig and annealing $YBa_2Cu_3O_{7-\delta}$ single crystals [13]. Similarly, the fishtail seen in $Ba(Fe_{1-x}Co_x)_2As_2$ is strongly suppressed after annealing [14].

In this article, we report a detailed study of the vortex creep in $Ca_{10}(Pt_4As_8)((Fe_{1-x}Pt_x)_2As_2)_5$ ($x \approx 0.05$) single crystals with $T_c = 26$ K. This compound belongs to the $Ca_{10}(Pt_nAs_8)((Fe_{1-x}Pt_x)_2As_2)_5$ family corresponding to $n = 4$ (10-4-8) [15–17]. Unlike other Fe-based superconductors, superconductivity, with the highest $T_c \sim 38$ K, occurs in 10-4-8 without chemical doping [18, 19]. It is also characterized by a huge upper critical field (H_{c2}) with relatively high anisotropy [20]. For instance, an upper critical field of $H^c_{c2}(0) \sim 92$ T ($\mathbf{H}//c$-axis), and upper critical field anisotropy of $\gamma^{T\to 0} \approx 1$ and $\gamma^{T\to Tc} \approx 10$ have been reported for samples with $T_c \sim 26$ K [20, 21]. Considering the penetration depth $\lambda(0) \approx 300$ nm and $\xi(0) \approx 2$ nm [20], we can estimate the thermodynamic critical field $H_c(T = 0\ \mathrm{K}) = \Phi_0/(2\sqrt{2}\,\pi\lambda\xi) \approx 0.38$ T (with Φ_0 the magnetic flux quantum) and the depairing current density $J_0(T = 0\ \mathrm{K}) = cH_c/3\sqrt{6}\,\pi\lambda \approx 55\ \mathrm{MA\ cm^{-2}}$ (where c is the speed of the light). The temperature dependent γ introduces an uncertainty in *Gi*. If we consider the whole range $\gamma = 1$ to 10 for this compound, $Gi \approx 0.0001$–0.02.

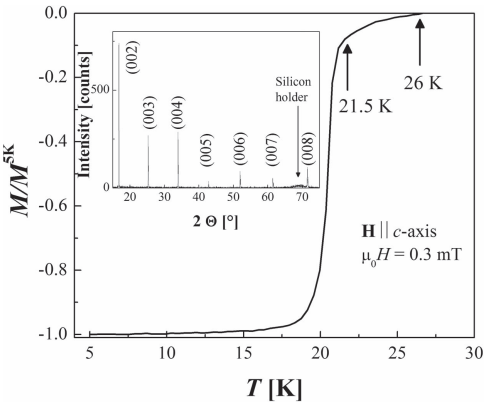

Figure 1. Temperature dependence of magnetization with $\mu_0 H = 0.3$ mT in the 10-4-8 crystal. The measurement was performed with $\mathbf{H}||c$- axis. Inset: x-ray diffraction pattern of the crystal showing the (00*l*) reflections.

2. Material and methods

The $Ca_{10}(Pt_4As_8)((Fe_{1-x}Pt_x)_2As_2)_5$ ($x \approx 0.05$) crystals were grown by the flux method [22]. For the magnetization measurements, we choose a rectangular-shaped plate with dimensions of 0.73 (length, l) × 0.7 (width, w) × 0.07 (thickness, t) mm^3, with c-axis parallel to t. The orientation of the crystal was verified by x-ray diffraction (see inset figure 1). The magnetization ($\mathbf{M}$) measurements were performed by using a superconducting quantum interference device (SQUID) magnetometer with the applied magnetic field ($\mathbf{H}$) parallel to the c-axis ($\mathbf{H}||c$). The T_c value (based on magnetization data) was determined from $M(T)$ at $\mu_0 H = 0.3$ mT applied after zero-field cooling (ZFC). The J_c was calculated from the magnetization data using the appropriate geometrical factor in the Bean Model. For $\mathbf{H}||c$, $J_c = \frac{20\Delta M}{w(1 - w/3l)}$, where ΔM is the difference in magnetization between the top and bottom branches of the hysteresis loop ($l > w$). The creep rate measurements were recorded for the period of time from 1 to 16 h. The magnetization of the sample holder was measured and subtracted from the data by averaging the initial points of the time relaxation for the lower and upper magnetic branches. Relaxation data correspond to the upper branch of the magnetization. The initial time was adjusted considering the best correlation factor in the log-log

fitting of the $\boldsymbol{J_c}(t)$ (for the first hour). The initial critical state for each creep measurement was generated using $\Delta H \sim 4H^*$, where H^* is the field for full-flux penetration [23]. Long-time flux creep relaxation measurements were fitted using the equation (2). A standard nonlinear fit using the Levenberg–Marquardt algorithm was applied. The fitted parameters were U_0, J_c, t_0 and μ. Due to the low influence of the first term of equation (2) in the fit, U_0 and J_c are correlated.

3. Results and discussion

Figure 1 shows the temperature dependence of the magnetization (normalized with **M** at 5 K) under $\mu_0 H = 0.3$ mT after ZFC. The $T_c \sim 26$ K corresponds to the onset of the magnetization. The maximum decay of the magnetization occurs at ≈21.5 K, in agreement with zero resistance in transport measurements (not shown).

Figure 2(*a*) shows the field dependence of J_c obtained from the Bean critical state mode at different temperatures. The self-field J_c at 1.8 K is around 0.42 MA cm^{-2}, which corresponds to ∼0.7% of the J_0 ($T = 0$ K). Similar (J_c/J_0) ratio is usually observed in pristine single crystals of other IBS such as FeSe (≈0.6%) [5] and Co-doped $BaFe_2As_2$ (≈1%) [2, 24]. Low J_c/J_0 is expected for vortex pinning dominated by random disorder [1]. The hysteresis loops for temperatures between 1.8 and 17.5 K display a SPM (see the inset of figure 2(*a*)), which moves towards lower fields as temperature increases. As mentioned above, the SPM is usually attributed to weak pinning [2, 3, 11]. A distinctive feature of the $J_c(H)$ at different temperatures is the strong enhancement in J_c below 5 K, which takes place in the same range of temperature where a reduction in γ from 2 to 1 is observed [20]. More detailed information of J_c (T) for different fields is shown in figure 2(*b*). Note that J_c increases dramatically below 5 K. For example, J_c at $\mu_0 H = 0.1$ T increases by about three times when the temperature is decreased from 5 K ($T/T_c \approx 0.2$) to 1.8 K ($T/T_c \approx 0.072$). This suggests that the increment in H_{c2} and the reduction in γ at $T < 5$ K produce an increment in $J_c(T)$.

Figure 3(*a*) shows a comparison between $J_c(H)$ and $S(H)$ for $T = 1.8$ K and $T = 7.5$ K. The S is obtained by measurements during the first 1 h. The $S(H)$ displays a maximum around the lower end of the fishtail (the minimum in $J_c(H)$), then decays as $J_c(H)$ increases, and finally increases rapidly above the SPM. The latest regime corresponds to plastic relaxation (related to fast creep) [2, 3]. Below the SPM, the $J_c(H)$ modulation can be explained by considering crossover between a single vortex regime (SVR) (negligible inter-vortex interaction) and vortex bundles in a week pinning scenario [11]. In addition, mixed pinning landscapes (including a low density of nanoparticles and random disorder) have been considered [25]. Continuous evolution in $\mu(H)$ (instead of discrete values) is commonly observed [2, 26]. The value of magnetic relaxation rate S varies from values as larger as 0.06 (at low fields) to $S \approx 0.02$ (at the SPM), which are consistent with previous observation in other IBS such as $Ba_{1-x}K_xFe_2As_2$ and Co-doped $BaFe_2As_2$ [8, 9, 24, 27]. Figure 3(*b*) shows the

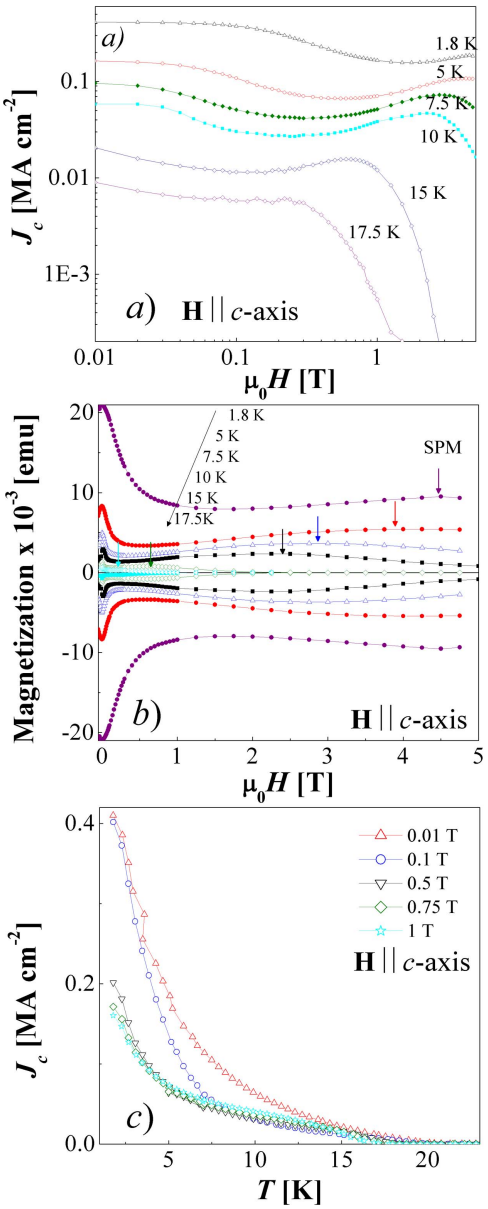

Figure 2. (a) Critical current density (J_c) versus magnetic field (H) at different temperatures (1.8, 5, 7.5, 10, 15 and 17.5 K). (b) Magnetization loops (positive magnetic fields) at several temperatures (the SPM is indicated by arrows). (c) Critical current density (J_c) versus temperature (T) at different magnetic fields (0.01, 0.1, 0.5, 0.75 and 1 T). All the measurement were performed with **H**||*c*-axis.

temperature dependence of the flux creep rate S at fields of $\mu_0 H = 0.1$, 0.3 and 1 T. Measurements were performed over 1 h duration. The $S(T)$ at the different fields displays a modulation that can be attributed to evolution in the vortex-bundle size due to the reduction of field for the SPM. Although non-negligible S is expected at $T \to 0$ K from quantum creep [28], it can be masked in small fields by self-field effects [11]. For 10-4-8 superconductor, noticeable large S is observed even at temperatures as low as 1.8 K. This fact reflects very small pinning energy U (see equation (3)). The crossover to fast creep (related to plastic creep) is evidenced at high temperatures (see arrows in figure 3(*b*)) [14].

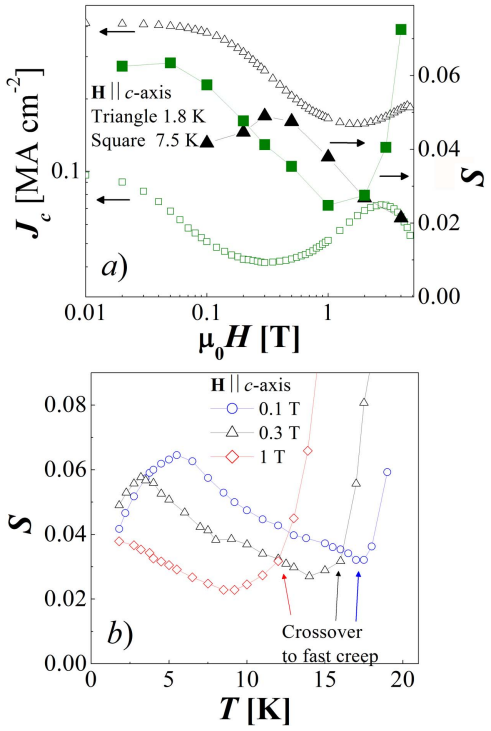

Figure 3. (a) Magnetic field dependence of J_c and the creep rate (S) at 1.8 and 7.5 K. (b) Creep rate (S) versus temperature (T) with μ_0H = 0.1, 0.3 and 1 T. All the measurements were performed with **H**||c-axis.

The characteristic *glassy exponent* μ at different regimes is usually estimated from Maley's method [29]. However, for samples with a SPM, it is expected to depend on the field and temperature ($\mu(H, T)$). We can obtain μ values through equation (2) in the glassy regime [11]. Relaxations for temperatures between 1.8 and 10 K were recorded over the period up to 16 h. In figures 4(a) and (c) we plot data as J versus t for $T = 5$ K and $T = 7.5$ K, respectively. Our results show that below the SPM (where elastic creep it is expected) the relaxation can be divided into two different regions. Region I corresponds to the field range where μ can be obtained by fitting data to equation (2) (fields smaller than the lower end of the SPM). Region II corresponds to the field range where the equation (2) is no longer valid (fields larger than the lower end and the SPM). In the latter regime, noticeable suppression in the long-time flux creep relaxation is observed. This phenomenon occurs in the field range where $S(H)$ reaches the minimum (see figure 3(a)), and it is usually attributed to small bundles with μ close to 3/2 [11].

Figures 4(b) and (d) show the field dependence of J_c and the corresponding μ values. Our results at low fields (Region I) are similar to those previously published in YBCO [11]. The μ value varies from 0.35 to more than 1 (i.e. $\mu = 1.22$ for $T = 7.5$ K and $\mu_0 H = 1$ T). The parameter t_0 obtained in the different fits is in the range 10^{-8}–10^{-10} [23]. Usually μ values which ranges between 0.7 and ≈1.6 are observed in pristine single crystals of different IBS, which include FeSe [4, 5], $FeTe_{0.6}Se_{0.4}$ [30] and Co-doped $BaFe_2As_2$ [14], among others. At low fields, μ is larger than that predicted for the SVR ($\mu = 1/7$), but comparable with that obtained in YBCO single crystals [11]. Single-vortex collective pinning is expected as long as $\gamma\ L_c <$ inter-vortex distance (a_0) (L_c is the Larkin length $L_c^c = \gamma^{-1}\xi\left(\frac{J_0}{J_c}\right)^{1/2}$). Above $\gamma\, L_c \approx a_0$, an increment in μ slows the relaxation down and the vortices begin to interact, leading to the first crossover to small bundles is expected ($\mu = 3/2$–$5/2$), then the second crossover to large bundles ($\mu = 7/9$) [1]. Similar analysis (including elastic and plastic regimes) has been applied to many superconducting systems in which the maximum at the SPM is considered as a crossover from elastic to plastic relaxation [2, 3, 8–11, 31–33]. The crossover between SVR and small vortex bundles (in anisotropic superconductors with **H**||c) is expected at $B_{sb} = \beta_{sb}\frac{J_c}{J_0}H_{c2}$, with $\beta_{sb} \approx 5$. Considering $J_c/J_0 \approx 0.007$ for $H_{c2}(0) \approx 90$ T [20], the SVR for 10-4-8 superconductor should be extended to $\mu_0 H \approx 3$ T at 0 K. When temperature is increased, the SVR is expected to be strongly suppressed by thermal fluctuations.

We now turn to Region II. This regime appears above 2 T at 1.8 K and is reduced with increasing temperature (i.e. $\mu_0 H \approx 1$ T is observed at 10 K). The outstanding feature is a temporal and gradual reduction in the $S(t)$ outside the predicted collective creep model. To determine the temporal variation in S, $J_c(t)$ is divided in fragments of 1 h and S is calculated within each fragment. Figure 5 shows the obtained result. A strong reduction in $S(t)$ is observed. This decay cannot be explained by considering the temporal evolution of $\ln(t/t_0)$. For example, considering $t_0 \approx 10^{-6}$–10^{-10} [23] and $\mu = 1$–2, in the limit $U_0 \ll \mu T \ln t/t_0$ (maximum temporal dependence), variation is expected to be smaller than 10% (see figure 5). However, our experimental results evidence changes over 50% in most cases. It is worth noting that S lower than 0.005 is observed at particular field and temperature (i.e. 3 T and 5 K) for period longer than 10 h.

The presence of the unexpected long-time relaxation in Region II can be understood by considering a stable vortex lattice configuration. As mentioned above, the SPM is related to an order–disorder transition (ODT) in the vortex lattice and the coexistence of ordered–disordered vortex structure [12, 34]. The coexistence of plastic (dislocation movement) and elastic motion should give rise to a stable vortex lattice configuration with better adjustment to the quenched disorder (random point defects). This scenario is consistent with previous results obtained in $YBa_2Cu_3O_{7-\delta}$ single crystals, in which a more disordered pinned state can be induced by shaking the vortex lattice with asymmetric AC fields [35]. The ODT may occur in the SVR or in the bundle pinning depending on the strength of the pinning potential and the magnitude of the thermal fluctuations (determined by the feasibility to generate dislocations in the vortex lattice) [12]. Considering that the root–mean square thermal fluctuation of the vortex lattice can be estimated by $\langle u^2 \rangle = c_L^2 a^2$ (where a is the inter-vortex distance and c_L is the phenomenological Lindeman constant ≈0.2) and a parameter $D = \xi(0)/\gamma L_c(0)$, the ODT takes place within the SVR if $D > c_L$, and above the SVR if $D < c_L$ [12]. For the studied system, $D \approx 0.08 < 0.2$ (small disorder), which is in agreement with the SPM above

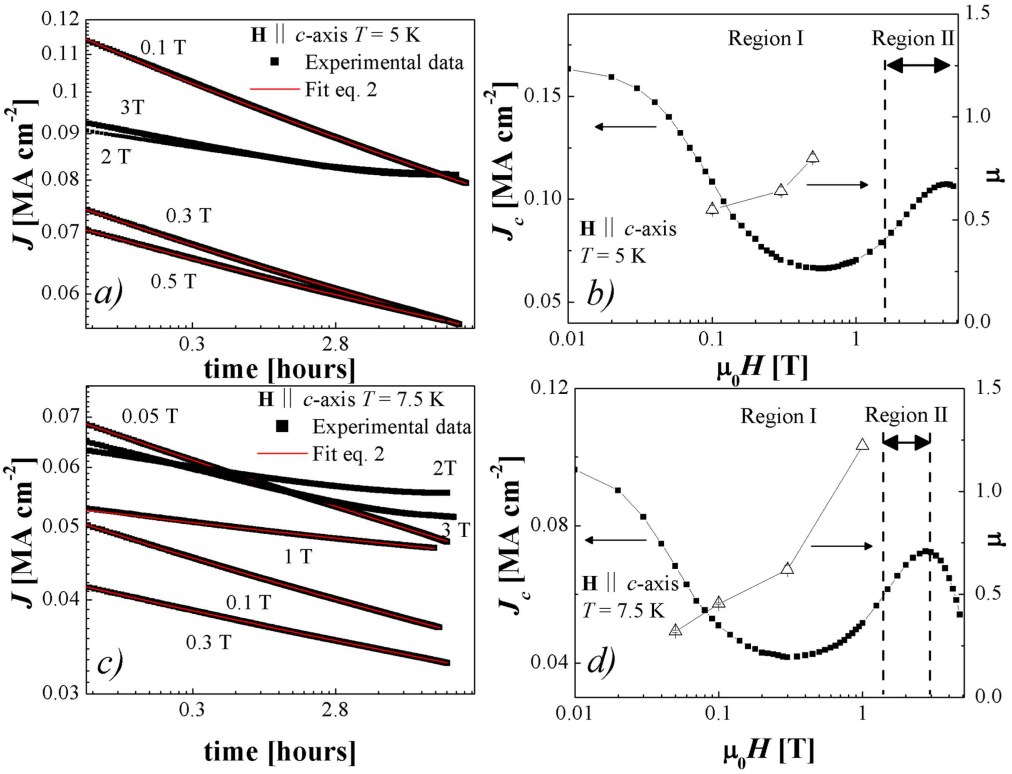

Figure 4. (a) and (c) Long-term relaxations on the 10-4-8 crystal at 5 K and 7.5 K, respectively. (b) and (d) Magnetic field dependence of J_c and the μ values at 1.8 K and 7.5 K, respectively. Region I corresponds to the field range where equation (2) is valid. Region II corresponds to the field range where equation (2) cannot be applied.

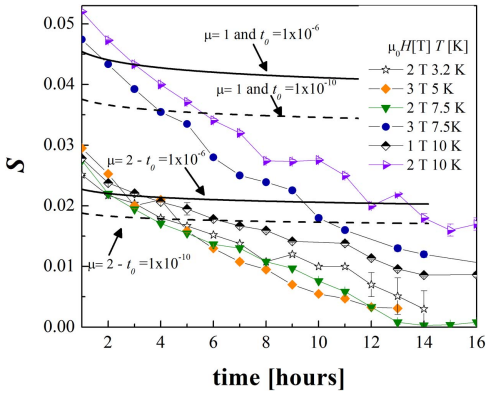

Figure 5. Flux creep rate (S) obtained in interval of 1 h for time between 1 and 16 h. The $S(t)$ dependence predicted by equation (2) as $S \approx [1/\mu \ln (t/t_0)]$ are also included.

the SVR. It is important to mention that the anomalous $H_{c2}(T)$ dependence observed in the $Ca_{10}(Pt_4As_8)((Fe_{1-x}Pt_x)_2As_2)_5$ [20] should have a relevant contribution to the ODT temperature dependence [12].

Through the above investigation, we demonstrate that the vortex dynamics of $Ca_{10}(Pt_4As_8)((Fe_{1-x}Pt_x)_2As_2)_5$ can be well described by weak collective pinning. Small U is expected from the high flux creep rate observed at low temperatures (manifested as huge flux creep rate). According to equation (3), $U_c \approx 10$–20 K using $S^{1.8\,K.,1\,T} = 0.038$, $\mu^{1.8\,K.,1\,T} = 0.8$ and $\ln (t/t0) \approx 30$. The $J_c(H)$ shows the typical $S(H)$ modulation, attributable to relaxation by vortex bundles and a crossover to fast creep (plastic relaxation). The flux creep rate below the SPM can be divided into two regions: (I) is at low and intermediate fields, where the rate is well described considering glassy relaxation with characteristic μ exponent that varies between 0.35 (at low fields) to values higher than 1 (at fields slightly larger than the minimum in J_c); (II) is at high fields (between the minimum and the SPM), where the relaxation cannot be analyzed by the collective creep model considering the equation (2). We observe small flux creep rate with $S < 0.01$, which could be related to the coexistence of elastic and plastic motion contributing to a stable disordered vortex lattice configuration in a pinning landscape dominated by random disorder. Considering that the field position of the SPM can be adjusted by modifying the quenched potential (i.e. modifying (J_c/J_0) by irradiation), our results suggest that extremely low flux creep relaxation rate can be tuned.

4. Conclusions

We have studied the vortex dynamics of $Ca_{10}(Pt_4As_8)((Fe_{1-x}Pt_x)_2As_2)_5$ single crystals with $T_c = 26$ K by performing magnetization measurements. The field dependence of the magnetization displays a SPM, which is associated with weak pinning produced by random disorder and chemical inhomogeneities. A state with strong reduction in the flux creep rate is observed (between the minimum and the SPM). Considering that the field position of the SPM can be adjusted

by modifying the quenched potential (i.e. modifying (J_c/J_0) by irradiation), our results suggest that extremely low flux creep relaxation rate may be tuned in many other superconducting materials.

Acknowledgments

This work has been partially supported by Agencia Nacional de Promoción Científica y Tecnológica PICT 2015-2171. N H is member of the Instituto de Nanociencia y Nanotecnología CNEA-CONICET (Argentina). Research at LSU (S H and R J) is financially supported by US NSF via the grant no. DMR-1504226.

ORCID iDs

N Haberkorn https://orcid.org/0000-0002-5261-1642
R Jin https://orcid.org/0000-0001-5846-4324

References

[1] Blatter G *et al* 1994 *Rev. Mod. Phys.* **66** 1125
[2] Prozorov R *et al* 2008 *Phys. Rev.* B **78** 224506
[3] Abulafia Y *et al* 1996 *Phys. Rev. Lett.* **77** 1596
[4] Sun Y, Pyon S, Tamegai T, Kobayashi R, Watashige T, Kasahara S, Matsuda Y and Shibauchi T 2015 *Phys. Rev.* B **92** 144509
[5] Amigó M L, Haberkorn N, Pérez P D, Suárez S and Nieva G 2017 *Supercond. Sci. Technol.* **30** 125017
[6] Senatore C *et al* 2008 *Phys. Rev.* B **78** 054514
[7] van der Beek Cornelis J, Konczykowski M, Kasahara S, Terashima T, Okazaki R, Shibauchi T and Matsuda Y 2010 *Phys. Rev. Lett.* **105** 267002
[8] Shen B *et al* 2010 *Phys. Rev.* B **81** 014503
[9] Salem-Sugui S *et al* 2010 *Phys. Rev.* B **82** 054513
[10] Wei Z, Xiangzhuo X, Wenjuan W, Haijun Z and Zhixiang S 2016 *Sci. Rep.* **6** 22278
[11] Civale L, Krusin-Elbaum L, Thompson J R and Holtzberg F 1994 *Phys. Rev.* B **50** 7188
[12] Mikitik G P and Brandt E H 2001 *Phys. Rev.* B **64** 184514
[13] Oka A, Koyama S, Izumi T, Shiohara Y, Shibata J and Hirayama T 2000 *Japan. J. Appl. Phys.* **39** 5822
[14] Haberkorn N, Jeehoon K, Gofryk K, Ronning F, Sefat A S, Fang L, Welp U, Kwok W L and Civale L 2015 *Supercond. Sci. Technol.* **28** 055011
[15] Ni N, Allred J M, Chan B C and Cava R J 2011 *Proc. Natl. Acad. Sci. USA* **108** E1019
[16] Kakiya S *et al* 2011 *J. Phys. Soc. Jap.* **80** 093704
[17] Löhnert C *et al* 2011 *Angew. Chem. Int. Ed.* **50** 9195
[18] Kakiya S *et al* 2011 *J. Phys. Soc. Japan* **80** 093704
[19] Tobias S, Gerald D and Dirk J 2012 *Phys. Rev.* B **86** 060516
[20] Mun E *et al* 2012 *Phys. Rev.* B **85** 100502
[21] Ding Q-P *et al* 2012 *Phys. Rev.* B **85** 104512
[22] Jiayun P, Amar K, Plummer E W and Rongying J 2017 *J. Phys.: Condens. Matter* **29** 485702
[23] Yeshurun Y, Malozemoff A P and Shaulov A 1996 *Rev. Mod. Phys.* **68** 911
[24] Haberkorn N, Maiorov B, Usov I O, Weigand M, Hirata W, Miyasaka S, Tajima S, Chikumoto N, Tanabe K and Civale L 2012 *Phys. Rev.* B **85** 014522
[25] van der Beek C J *et al* 2010 *Phys. Rev.* B **81** 174517
[26] Thompson J R, Sun Y, Christen D, Civale L, Marwick A and Holtzberg F 1994 *Phys. Rev.* B **49** 13287
[27] Taen T, Ohtake F, Pyon S, Tamegai T and Kitamura H 2015 *Supercond. Sci. Technol.* **28** 085003
[28] Klein T, Grasland H, Cercellier H, Toulemonde P and Marcenat C 2014 *Phys. Rev.* B **89** 014514
[29] Maley M P, Willis J O, Lessure H and McHenry M E 1990 *Phys. Rev.* B **42** 2639
[30] Yue S *et al* 2013 *Europhys. Lett.* **103** 57013
[31] Haberkorn N, Eom M J, Sang Y J, Jeehoon K and Sung K J 2016 *Solid State Commun.* **231–232** 26
[32] Klein T *et al* 1998 *Europhys. Lett.* **42** 79
[33] Yanjing J, Wang C, Qiang D, Huan Y and Hai-Hu W 2018 *Physica* C **545** 43–9
[34] Marchevsky M, Higgins M J and Bhattacharya S 2000 *Nature* **403** 398
[35] Valenzuela S and Bekeris V 2001 *Phys. Rev. Lett.* **86** 504